Ammonium-Assisted Intercalation of Java Bentonite as Effective of Cationic Dye Removal

Yusuf Mathiinul Hakim[1], Risfidian Mohadi[2*], Mardiyanto[3], Idha Royani[4]

[1] Graduate School, Faculty of Mathematics and Natural Sciences, Sriwijaya University, Palembang, 30139, Indonesia

[2] Department of Chemistry, Faculty of Mathematics and Natural Sciences, Sriwijaya University, Palembang, 30139, Indonesia

[3] Pharmaceutical Department, Faculty of Mathematics and Natural Sciences, Sriwijaya University, Palembang, 30139, Indonesia

[4] Department of Physics, Faculty of Mathematics and Natural Sciences, Sriwijaya University, Palembang, 30139, Indonesia

* Corresponding author's e-mail: risfidian.mohadi@unsri.ac.id

ABSTRACT

Modification of Java bentonite assists by the multi-step intercalation of sodium and ammonium ions under low-temperature preparation. The adsorbent was examined to remove rhodamine B and methylene blue dyes in an aqueous solvent. The analysis of structural changes conducted by XRD analysis showed the peak shifting from 19.89° to 16.1° and specific peak spectra FTIR of 2846.93 cm^{-1} due to increase basal spacing from ammonium intercalation. The total capacities of NH-bentonite, Na-bentonite, and Natural Bentonite adsorption to rhodamine B were 192.308 mg/g, 136.936 mg/g, and 116.279 mg/g, respectively, under acidic conditions. Furthermore, the total capacities of NH-bentonite, Na-bentonite, and Natural Bentonite adsorption to methylene blue were 270.27 mg/g, 158.73 mg/g, and 136.986 mg/g, respectively, under alkaline conditions. The adsorption mechanism described that the rhodamine B and methylene blue removal occurred endothermically, was feasible, and adhered to the kinetics model of pseudo-second-order and Langmuir isotherm. It concluded that the modified Java Bentonite from multi-step intercalation is affordable and effective as wastewater treatment.

Keywords: bentonite intercalation, ammonium intercalant, adsorption, rhodamine b, methylene blue.

INTRODUCTION

Contamination of the aquatic ecosystem has become an urgent concern due to the accumulation of pollutant inside it. Dye waste plays a large role in product coloring which pollutes in wide-area of the aquatic ecosystem due to annually discharged without proper treatment by industries (Tkaczyk et al., 2020). The complex structure of dye waste triggers accumulation in the environment and is difficult to degrade with traditional treatment (Khattab et al., 2020; Mahmoudabadi et al., 2019). The cationic dyes are extensively used in the coloring-needed industry, especially rhodamine B (RhB) and methylene blue (MB) with the structure shown in Figure 1 (Gupta et al., 2004; Rochkind et al., 2014). Naturally, the group of cationic dyes that classes to thiazine (for RhB) and xanthate (for MB) are considered more toxic due to their positive charge that easily interacts with organic life cells (Gillman, 2011; Inyinbor et al., 2015).

Nowadays, innovations in treatment techniques and materials include cation/anion exchange (Pai et al., 2021), biodegradation (Varjani et al., 2020), chemical coagulation (Iwuozor, 2019), catalyst reduction (Menon et al., 2021), adsorption (Rápó et al., 2020), and hybrid materials are proposed (Imgharn et al., 2022). Adsorption was established as a favorable technique because of its simplicity, low cost, and effectiveness (Crini,
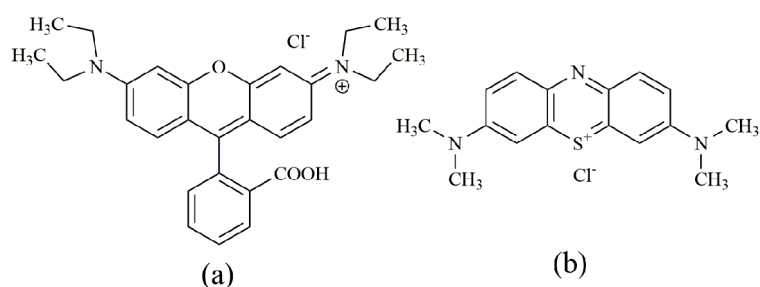
Figure 1. Chemical Composition of RhB (a) and MB (b)

2006; Yang et al., 2022). Popular adsorbents that are generally used include activated carbon, graphene, zeolites, polymers, layered double hydroxides, and clay-bentonite (Funes et al., 2020; H. Liu et al., 2022; Q. Liu et al., 2022; Maharana & Sen, 2021; Sharma et al., 2022; Zhong et al., 2022).

Natural material improvement has been raised as an urgent research topic for obtaining an eco-friendly material for wastewater treatment. Recently, raw materials from household wastes, agricultural products, industrial waste, marine materials, and soil are transformed to obtain an effective adsorbent (Pourhakkak et al., 2021). Bentonite is included in the clay mineral in the soil structure and is abundant in nature. Clay minerals are classified based on their minerals, including sepiolite (Gao et al., 2022), palygorskite (Câmara et al., 2020), zeolite (Sudibandriyo & Putri, 2020), kaolinite (Şenol et al., 2022), and bentonite (Wang et al., 2022). Bentonite is a type of smectite multilayer of octahedra alumina-silica tetrahedra which consist of montmorillonite mineral and others. The space between the layers contains exchangeable cations, including Cu^{2+}, Mg^+, Na^+, K^+, and others, thus usually improving into multifunctional material, especially adsorbent (Andrunik & Bajda, 2019).

Several innovations to improve bentonite capacity adsorption are acid activation (Adane et al., 2022), high-temperature activation (Rehman et al., 2019), cold plasma treatment (Hidalgo-Herrador et al., 2017), composites (Italiya et al., 2022), and pillarization/intercalation (Barakan & Aghazadeh, 2021; Funes et al., 2020). Recently, Islam & Mostafa (2022) examined the capacity of natural bentonite adsorption on MB removal at 25.19 mg/g. The research conducted by Teğin & Saka (2021) reported thermal activation clay under high temperature which then gained the highest adsorption capacity of MB at 21.27 mg/g. According to de Morais Pinos et al. (2022) and

Malsawmdawngzela et al. (2021), bentonite-modified organic polymers (surfactant cetyltrimethylammonium and mercaptopropyltrimethoxysilane, respectively) show the capacity of RhB adsorption at 0.98 mg/g and 16.42 mg/g, respectively. He et al. (2022) reported that the composites of organic bentonite-kaolin have the highest RhB adsorption capacity at 12.68 mg/g.

This work focused on bentonite modification by multi-step intercalation under low temperatures preparation assisted by sodium and ammonium ions. Bentonite-modified was examined as dyes waste removal in the case of RhB and MB. The mechanism of adsorption was analyzed by the following parameters: the pH effect, adsorption time, kinetics, isotherm, and thermodynamics adsorption. Furthermore, the conformed bentonite adsorbent prepared and modified based on the natural ambiance was proposed as an economical adsorbent in wastewater management.

MATERIAL AND METHODS

Chemical and instrumentation

The specific Java Bentonite was purchased from Bentonit Makmur Sentosa Company in East Java of Indonesia with further treatment (sun-dried for 1 hour and filter-sieved in 200 mesh). The chemicals are Sigma Aldrich production in pure grade used without prior purification: sodium chloride (NaCl), ammonium chloride (NH_4Cl), hydrochloric acid (HCl), sodium hydroxide (NaOH), distilled water, rhodamine B, and methylene blue. The characterization was conducted by using X-Ray Rigaku Miniflex-600 Diffractometer, FT-IR Spectrophotometer type Shimadzu Prestige-21, and UV-Visible Bio-base Spectrophotometer BKUV1800PC.

Bentonite intercalation

The Java Bentonite intercalated was prepared in steps: 100 g of bentonite was homogenized in 333 mL of saturated NaCl at 25 °C for 120 minutes, then dissolved in aqua solvent (the ratio of the mixture and solvent is 1:2, respectively) for 10 minutes. The mixture was filtered; then, the bentonite was re-homogenized in 333 mL of saturated NaCl at 25 °C for 120 minutes. The bentonite residue was washed using boiled water three times, then oven-dried at 200 °C for 12 hours. The product was named Na-bentonite.

In further steps, the 50 g of Na-bentonite was homogenized in 165 mL of saturated NH_4Cl at 25 °C for 120 minutes and dissolved with aqua solvent (the ratio of the mixture and solvent is 1:2, respectively) for 10 minutes. The deposits were filtered and re-homogenized in 165 mL of saturated NH_4Cl at 25 °C for 120 minutes. The deposit materials were washed three times using boiled water and oven-dried at 200 °C for 12 hours. The product was named NH-bentonite.

Adsorption work

Several parameters were examined as the effect of pH variation and the adsorption time by varying the pH adsorbate of 2, 3, 4, 5, 6, 7, 8, 9, 10, and 11, then the adsorption time of 0, 10, 20, 30, 40, 50, 60, 70, 80, 90, 100, 120, and 150 minutes. The adsorption process was started by mixing 50 mg/L dye solution with 0.02 g adsorbent in the beaker. The sample concentration after adsorption was analyzed by UV-Visible spectrophotometer using the specific wavelength of RhB at 555 nm and MB at 665 nm. Furthermore, the effects of temperature and initial concentration of adsorption were studied by varying the temperature of 30, 40, 50, 60, and 70 °C, then the initial concentration for RhB of 50, 75, 100, 125, and 150 mg/L and for MB of 250, 255, 260, 265, and 270 mg/L (the different range due to effectiveness dye adsorption according to the preliminary trial).

Mechanism adsorption analysis

The quantity of RhB and MB adsorbed is calculated by the formula:

$$q_t = \frac{(C_0 - C_t)v}{m} \qquad (1)$$

where: q_t – the total of sample adsorbed at a specific time (mg/g);
C_0 and C_t – sample concentration at initial and specific time adsorption (mg/L);

v – the volume of sample adsorption (mL);
m – the amount of adsorbent (g).

The kinetic adsorption was analyzed by pseudo-first-order (PFO) (2) and pseudo-second-order (PSO) (3) models that were determined by the formula:

$$log(q_t - q_e) = \log q_t - \frac{K_1 t}{2.303} t \qquad (2)$$

$$\frac{t}{q_t} = \frac{1}{K_2 q_t^2} + \frac{1}{q_t} t \qquad (3)$$

where: q_t and q_e – the total of sample adsorbed at a specific time and equilibrium phase (mg/g);
K_1 – the adsorption rate constant of the PFO models (min^{-1});
K_2 – the adsorption rate constant of the PSO models (min^{-1}).

The isotherm adsorption models were conducted to Langmuir (4) and Freundlich (5) models that were determined by the formula:

$$\frac{C_e}{q_e} = \frac{1}{q_{max}K_L} + \frac{C_e}{q_{max}} \qquad (4)$$

$$lnq_e = lnK_f + \frac{1}{n}lnC_e \qquad (5)$$

where: C_e – the sample concentration in the equilibrium phase (mg/L);
q_e and q_{max} – the total of sample adsorbed at the equilibrium phase and maximum condition (mg/g);
K_L – the constant of Langmuir adsorption (mg/L);
K_f (L/g) and n – the constant of Freundlich adsorption.

The thermodynamic adsorption was measured by the formula:

$$\Delta G° = -RTlnK_d \qquad (6)$$

$$lnK_d = \frac{\Delta S°}{R} - \frac{\Delta H°}{RT} \qquad (7)$$

$$K_d = \frac{q_e}{C_t} \qquad (8)$$

where: K_d – the adsorption distribution coefficient;
C_t – sample concentration at the equilibrium phase (mg/L);
q_e – the quantity of sample adsorbed at the equilibrium phase (mg/g);
R and T – the gas constants and absolute temperature (K).

RESULT AND DISCUSSION

The Bentonite-intercalated diffraction patterns displayed in Figure 2 showed that intercalation has changed the structure of Java Bentonite. Bentonite belongs to the smectite group with dominancy of montmorillonite minerals, which is confirmed by the reflections of 2θ around 5°, 20°, 35°, and 62° (Mao et al., 2021; Taher et al., 2018). Furthermore, the quartz minerals were detected at 26°, then feldspar reflections at 28° (Kumar & Lingfa, 2020).

The decreased impurities from quartz minerals are indicated by the decreased peak of 26° due to the different binding forces of NH_4^+ intercalant at NH-bentonite in Figure 2c (Salah et al., 2019). Shifting of peak denoted basal spacing (d_{001}) expected from the different 2θ of Natural Bentonite at 19.89° to Na-bentonite at 19.9° to NH-bentonite at 16.1° (Miyazaki et al., 2019).

FT-IR spectra of all bentonite-intercalated have no significant changes, showing stretch vibration of the interlayer O-H group at 3422 cm^{-1} and 1635 cm^{-1} (Wei et al., 2020). According to
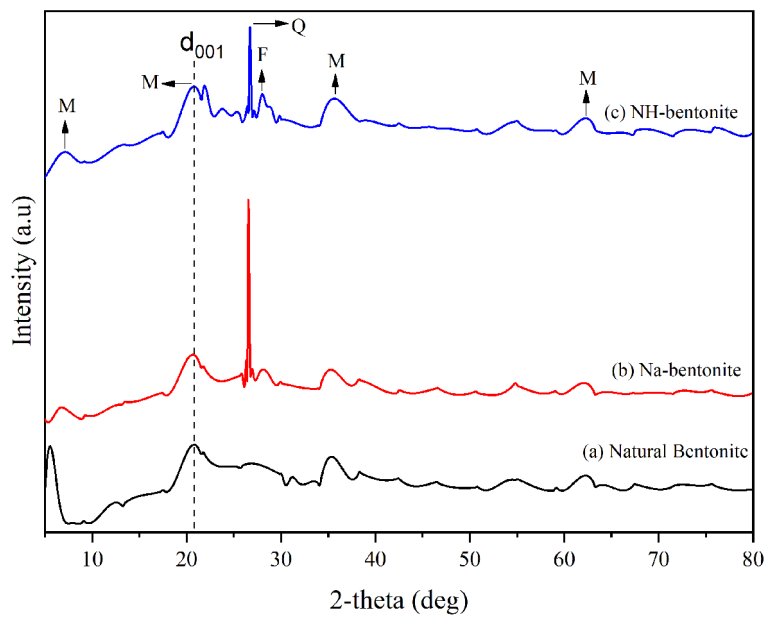

Figure 2. XRD spectra arrangement of bentonite intercalated (where M = montmorillonite, Q = quartz, and F = feldspar)
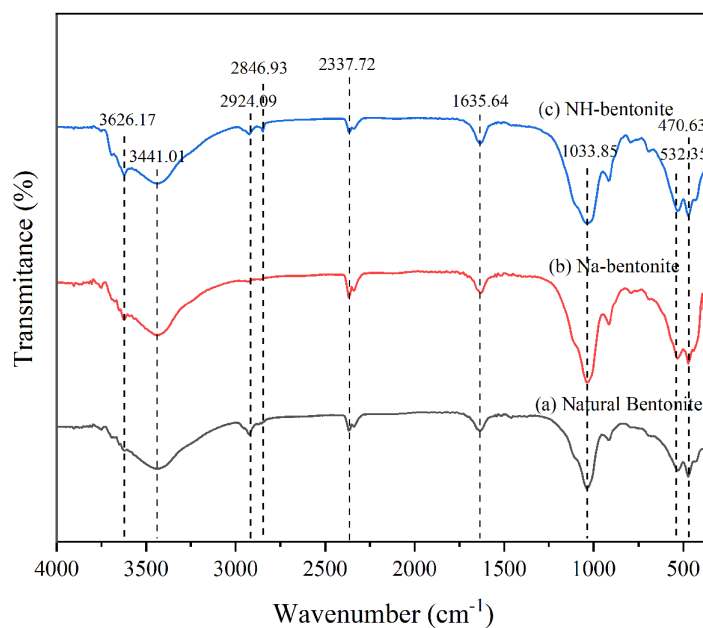

Figure 3. FT-IR spectra of bentonite intercalated

Taher et al. (2019), the standard spectra of bentonite minerals are 470 cm⁻¹, 532 cm⁻¹, 910 cm⁻¹, 1033 cm⁻¹, 1635 cm⁻¹, 3433 cm⁻¹, and 3749 cm⁻¹. Ammonium ions have inserted inside the layer of bentonite and detected at 2846.93 cm⁻¹ due to has better binding force with Si-O structure (Kloprogge, 2017; Pironon et al., 2003). The bentonite structures are stable according to the unchangeable

bands in the spectra since marked at 1033 cm⁻¹ denoted as the Si-O-Si vibrations (Taher et al., 2018), then the wavenumber of 470.63 cm⁻¹ and 532.35 cm⁻¹ denoted as the Al-Al-OH vibrations (Zaher MS et al., 2018).

The pH dyes were controlled by the range of 2-11 to achieve the optimum condition. On the basis of Figure 4, the equilibrium adsorption
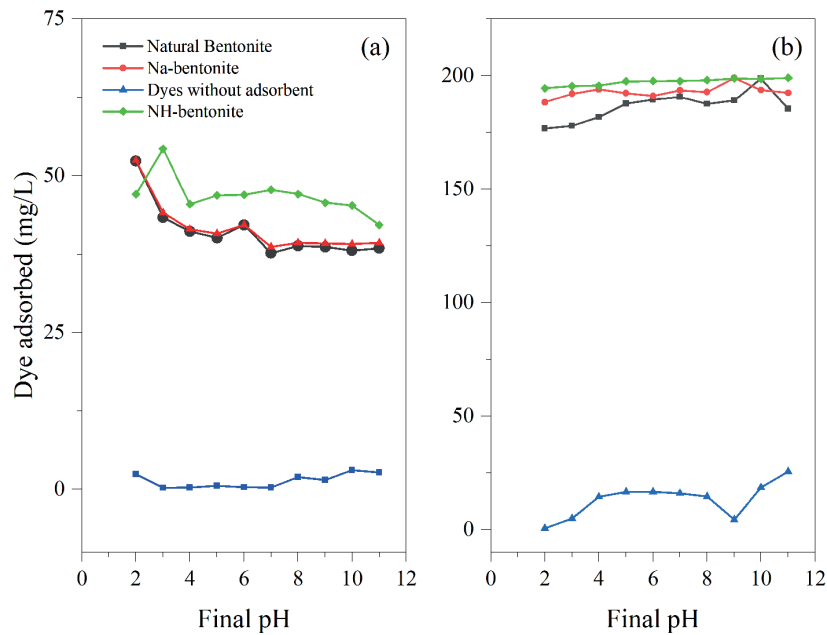

Figure 4. Effect of pH variation on adsorption of RhB (a) and MB
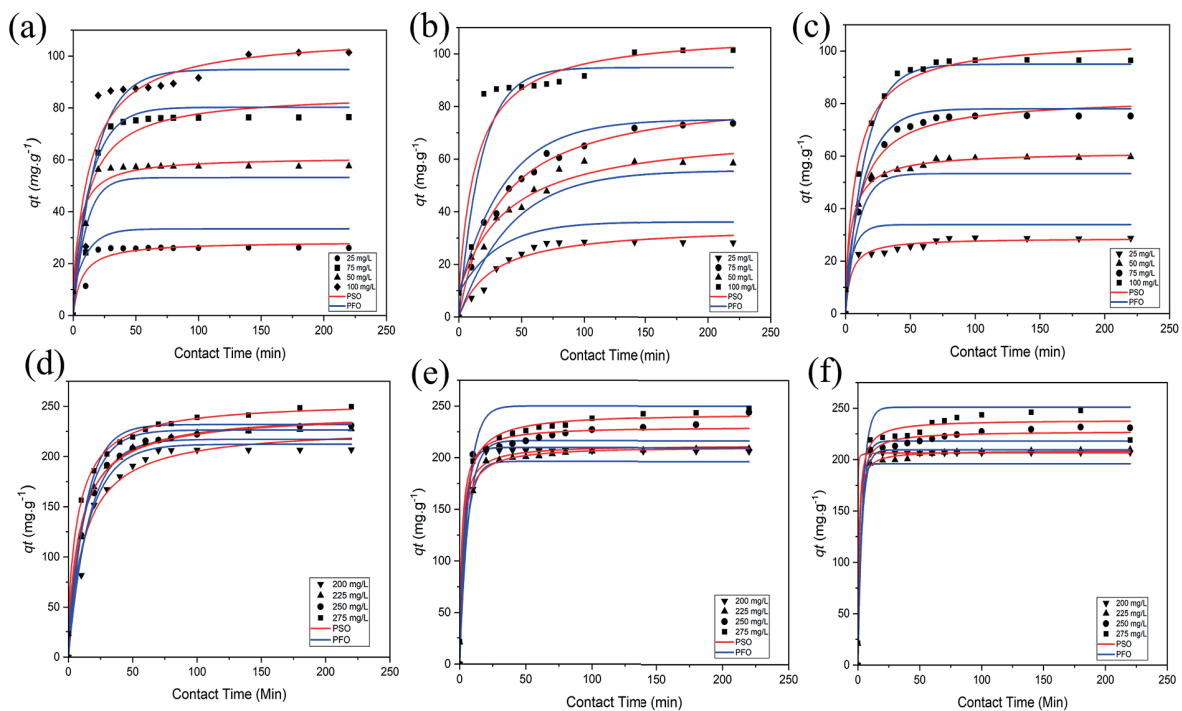(b) using natural bentonite, Na-bentonite, and NH-bentonite

Figure 5. The kinetics adsorption parameter of natural bentonite, Na-bentonite, and
NH-bentonite to RhB (a, b, and c, respectively) and MB (d, e, and f, respectively)

on Natural Bentonite, Na-bentonite, and NH-bentonite are compared to the pure dye concentration before adsorption with the optimum pH adsorption on RhB 2, 2, and 3, respectively, then the optimum pH adsorption on MB 9, 8, and 11, respectively. According to Ribeiro dos

Table 1. Adsorption Kinetic Parameters

| Dye	Adsorbent	Dye Conc. (mg.L^{-1})	PFO		PSO	
			K (min^{-1})	R^2	K (g.mg/min^{-1})	R^2
RB	Natural bentonite	25	0.108	0.7725	0.0119	0.9972
		50	0.03	0.5727	0.0085	0.9989
		75	0.039	0.7832	0.0019	0.9926
		100	0.033	0.8766	0.0004	0.9749
	Na-bentonite	25	0.069	0.8929	0.0055	0.9767
		50	0.023	0.9632	0.0004	0.9821
		75	0.024	0.9797	0.0003	0.9976
		100	0.022	0.9696	0.0003	0.9965
	NH-bentonite	25	0.035	0.8125	0.006	0.0087
		50	0.047	0.8877	0.004	0.9996
		75	0.079	0.9347	0.002	0.9985
		100	0.067	0.9731	0.0018	0.9986
MB	Natural bentonite	200	0.067	0.8875	0.0006	0.9972
		225	0.04	0.9675	0.0005	0.9995
		250	0.03	0.9235	0.0005	0.9999
		275	0.03	0.926	0.0004	0.9998
	Na-bentonite	200	0.063	0.5086	0.011	0.9999
		225	0.042	0.7479	0.002	1
		250	0.018	0.6108	0.0007	0.9983
		275	0.026	0.7395	0.0006	0.9996
	NH-bentonite	200	0.058	0.428	0.046	1
		225	0.046	0.7395	0.003	1
		250	0.025	0.6727	0.001	0.9998
		275	0.029	0.727	0.0008	0.9996
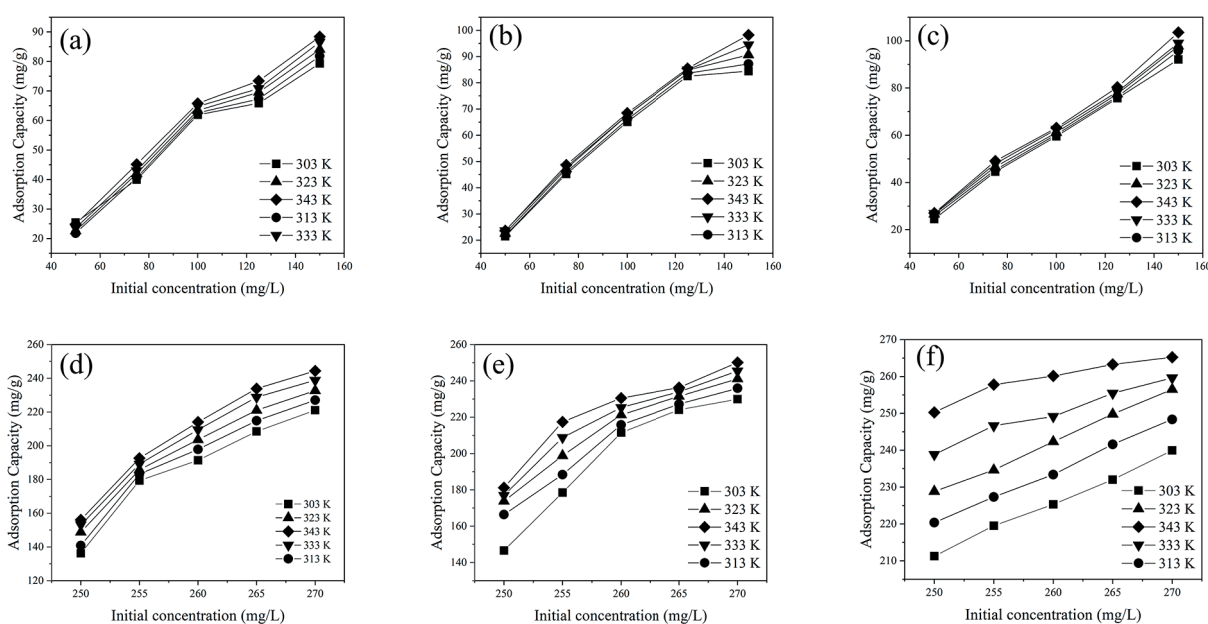
Figure 6. The trend of initial concentration and temperature variation on the adsorption of RhB (a, b, and c, respectively) and MB (d, e, and f, respectively) Using Natural Bentonite, Na-bentonite, and NH-bentonite

Santos et al. (2019),under acidic conditions RhB molecules are in the monomeric state; thus, the mechanism of adsorption driven by the RhB molecules easily enters the adsorbent pores. Moreover, the mechanism adsorption of MB occurs by electrostatic interaction and ion exchanges between MB molecules to ammonium and hydroxyl group on the adsorbent; thus, it is triggered under alkaline conditions and it is supported by previous research (Pandey & Ramontja, 2016; Shaarawy et al., 2020).

The time variation was analyzed to determine the equilibrium state of the kinetics adsorption models. Figure 5 shows the kinetic adsorption parameter of Natural Bentonite, Na-bentonite, and NH-bentonite on adsorption of RhB (a, b, and c) and MB (d, e, and f), the equilibrium state of the adsorption occurs at 100 minutes. The analysis of kinetics adsorption models was supported by the data in Table 1 and it can be concluded that the adsorption process of bentonite-intercalated adsorbent the pseudo-second-order (PSO) model

Table 2. Isotherm adsorption parameters

Dye	Adsorbent	Freundlich		Langmuir	
		$1/n$	R^2	Q_{max} (mg/g)	R^2
RB	Natural bentonite	2.896	0.8909	116.279	0.9776
	Na-bentonite	2.614	0.8495	136.986	0.981
	NH-bentonite	1.814	0.9626	192.308	0.9244
MB	Natural bentonite	2.847	0.9631	136.986	0.9867
	Na-bentonite	3.492	0.9865	158.730	0.9964
	NH-bentonite	52.632	0.4813	270.270	0.9999

Table 3. Thermodynamic adsorption of RhB using bentonite-intercalated

RB Conc.	T (K)	Natural bentonite			Na-bentonite			NH-bentonite		
		$\Delta H°$ (kJ/mol)	$\Delta S°$ (kJ/mol)	$\Delta G°$ (kJ/mol)	$\Delta H°$ (kJ/mol)	$\Delta S°$ (kJ/mol)	$\Delta G°$ (kJ/mol)	$\Delta H°$ (kJ/mol)	$\Delta S°$ (kJ/mol)	$\Delta G°$ (kJ/mol)
50 mg/L	303			-2.64			-3.68			-5.46
	313			-3.16			-4.16			-6.06
	323	12.93	0.051	-3.67	10.6	0.047	-4.63	12.72	0.06	-6.66
	333			-4.18			-5.10			-7.26
	343			-4.70			-5.57			-7.86
75 mg/L	303			-3.50			-4.48			-3.16
	313			-3.88			-4.93			-3.49
	323	7.96	0.038	-4.26	8.97	0.044	-5.37	6.743	0.033	-3.82
	333			-4.64			-5.82			-4.14
	343			-5.02			-6.26			-4.47
100 mg/L	303			-1.50			-4.15			-3.67
	313			-1.79			-4.46			-3.90
	323	7.35	0.029	-2.08	5.12	0.031	-4.77	3.261	0.023	-4.13
	333			-2.37			-5.07			-4.36
	343			-2.67			-5.38			-4.58
125 mg/L	303			-1.29			-1.66			-2.46
	313			-1.56			-2.11			-2.87
	323	6.99	0.027	-1.84	11.86	0.045	-2.55	10.21	0.042	-3.29
	333			-2.11			-3.00			-3.71
	343			-2.38			-3.45			-4.13
150 mg/L	303			-0.25			0.23			-1.57
	313			-0.58			-0.06			-2.00
	323	10	0.034	-0.92	9.22	0.030	-0.35	11.6	0.043	-2.43
	333			-1.26			-0.65			-2.87
	343			-1.60			-0.95			-3.30

indicated by the value of R² which is closer to 1. The pseudo-second-order models describe that adsorption occurs due to the interaction of adsorbent and adsorbates by chemisorption mechanism (Shattar & Foo, 2022; Toor & Jin, 2012). Furthermore, Figure 6 shows the data support of the removal ability by the adsorbent based on the data variation of temperature and concentration.

On the basis of the data of initial concentration and temperature variation on the adsorption of RhB and MB, it was confirmed that increasing temperature adsorption generated an increase in concentration adsorption. The highest adsorption capacity occurs at the temperature of 70 °C. Table 2 explained the analysis of isotherm adsorption parameters, the highest adsorption capacity of RhB and MB were reached by NH-bentonite with the value 192.308 mg/g and 270.270 mg/g, respectively. The adsorption process has adhered to the Langmuir isotherm equation, confirmed by the R² value being closer to 1 (Chopra et al.,

2012; Siregar et al., 2021). The Langmuir model described that the adsorption process was triggered by specific interaction between active site adsorbent to adsorbate and occurs in monolayer adsorption (Jović-Jovičić et al., 2008).

The analysis of thermodynamic adsorption of RhB and MB are shown in Tables 3 and 4, respectively. The adsorption using Natural Bentonite, Na-bentonite, and NH-bentonite was generated in the spontaneous condition that was indicated by negative values of Gibbs energy (Jedli et al., 2019). Furthermore, the adsorption happened by endothermic process and was feasible, which is confirmed by the positive value of enthalpy and entropy energy (Allaoui et al., 2020; Yoshida et al., 2020). According to Jabar et al. (2020) and Malima et al. (2021) if $\Delta H° < 20$ kJ/mol means the adsorption happened in physisorption and if the value of $\Delta H°$ between 40-120 kJ/mol means the adsorption happened in chemisorption.

Table 4. Thermodynamic adsorption of MB using bentonite-intercalated

MB Conc.	T (K)	Natural bentonite			Na-bentonite			NH-bentonite		
		$\Delta H°$ (kJ/mol)	$\Delta S°$ (kJ/mol)	$\Delta G°$ (kJ/mol)	$\Delta H°$ (kJ/mol)	$\Delta S°$ (kJ/mol)	$\Delta G°$ (kJ/mol)	$\Delta H°$ (kJ/mol)	$\Delta S°$ (kJ/mol)	$\Delta G°$ (kJ/mol)
250 mg/L	303			-0.42			-1.08			-2.95
	313			-0.68			-1.52			-5.33
	323	7.36	0.026	-0.93	12.40	0.044	-1.97	69.11	0.238	-7.70
	333			-1.19			-2.41			-10.09
	343			-1.44			-2.86			-12.47
255 mg/L	303			-2.04			-1.93			-2.96
	313			-2.28			-2.61			-5.40
	323	5.36	0.024	-2.53	18.63	0.068	-3.29	70.77	0.243	-7.83
	333			-2.77			-3.97			-10.26
	343			-3.01			-4.67			-12.7
260 mg/L	303			-2.52			-3.58			-3.40
	313			-2.97			-4.10			-5.79
	323	10.97	0.5	-3.41	12.16	0.052	-4.62	69.15	0.239	-8.19
	333			-3.86			-5.14			-10.58
	343			-4.30			-5.66			-12.97
265 mg/L	303			-3.15			-4.19			-4.25
	313			-3.76			-4.62			-6.08
	323	15.24	0.061	-4.37	8.742	0.043	-5.05	51.30	0.183	-7.91
	333			-4.98			-5.48			-9.74
	343			-5.58			-5.90			-11.58
270 mg/L	303			-3.58			-4.19			-4.88
	313			-4.19			-4.83			-6.11
	323	14.79	0.061	-4.80	15.29	0.064	-5.48	32.47	0.123	-7.35
	333			-5.40			-6.12			-8.58
	343			-6.01			-6.76			-9.81

Table 5. Comparison of Adsorption Capacity on Various Adsorbent

Adsorbent	Dye	Adsorption Capacity (mg.g⁻¹)	References
Fe-bentonite	RB	98.62	(Hou et al., 2011)
Al_2O_3-clay		52	(Yen Doan et al., 2020)
Cellulose-clay		40.9	(Kausar et al., 2021)
CTAB-bentonite		0.98	(de Morais Pinos et al., 2022)
Natural bentonite (Java Bentonite)		116.279	This study
Na-bentonite		136.986	
NH-bentonite		192.308	
Bentonite-hydroxyapatite	MB	175.4	(Vezentsev et al., 2018)
CTAB-bentonite		36.19	(Balarak et al., 2020)
Saudi Red Clay		50.25	(Khan, 2020)
Chitosan-Mmt/polyaniline		111	(Minisy et al., 2021)
Fe_3O_4-kaoline clay		18.78	(Hayoune et al., 2022)
Natural bentonite (Java Bentonite)		136.986	This study
Na-bentonite		158.73	
NH-bentonite		270.27	

This work is a proposed innovation to obtain a bentonite-based adsorbent that is effective on cationic dyes removal. Herethe comparison between the adsorption capacity of this work's adsorbent and another work's adsorbent is shown in Table 5. Table 5 confirms that the maximum adsorption capacity of NH-bentonite to RhB and MB in this study is greater than that of the adsorbents shown in Table 5.

CONCLUSIONS

The Java Bentonite modified by multi-step intercalation assisted by sodium and ammonium ions as intercalant under low-temperature preparation increased the basal spacing supports by the XRD analysis of increased basal spacing indicated by a shift of 2θ from 19.89° to 16.1°. Under the optimum conditions of the acidic pH, the capacity of NH-bentonite, Na-bentonite, and Natural Bentonite adsorption to RhB reach 192.308 mg/g, 136.936 mg/g, and 116.279 mg/g, respectively, then under the alkaline conditions, the capacity of NH-bentonite, Na-bentonite, Natural Bentonite adsorption to MB reach 270.27 mg/g, 158.73 mg/g, and 136.986 mg/g, respectively.

Acknowledgements

REFERENCES

1. Adane, T., Hailegiorgis, S.M., Alemayehu, E. 2022. Acid-activated bentonite blended with sugarcane bagasse ash as low-cost adsorbents for removal of reactive red 198 dyes. Journal of Water Reuse and Desalination. https://doi.org/10.2166/wrd.2022.056

2. Allaoui, S., Naciri Bennani, M., Ziyat, H., Qabaqous, O., Tijani, N., Ittobane, N. 2020. Kinetic Study of the Adsorption of Polyphenols from Olive Mill Wastewater onto Natural Clay: Ghassoul. Journal of Chemistry, 2020, 1–11. https://doi.org/10.1155/2020/7293189

3. Andrunik, M., Bajda, T. 2019. Modification of bentonite with cationic and nonionic surfactants: Structural and textural features. Materials, 12(22). https://doi.org/10.3390/ma12223772

4. Barakan, S., Aghazadeh, V. 2021. The advantages of clay mineral modification methods for enhancing adsorption efficiency in wastewater treatment: a review. Environmental Science and Pollution Research, 28(3), 2572–2599. https://doi.org/10.1007/s11356-020-10985-9

5. Câmara, A.B.F., Sales, R.V., Bertolino, L.C., Furlanetto, R.P.P., Rodríguez-Castellón, E., de Carvalho, L.S. 2020. Novel application for palygorskite clay mineral: a kinetic and thermodynamic assessment of

diesel fuel desulfurization. Adsorption, 26(2), 267–282. https://doi.org/10.1007/s10450-019-00144-z

6. Chopra, M., Drivjot, Amita. 2012. Adsorption of Dyes from Aqueous Solution Using Orange Peels: Kinetics and Equilibrium Studies. Journal of Advanced Laboratory Research in Biology, 3(1), 1–8.

7. Crini, G. 2006. Non-conventional low-cost adsorbents for dye removal: A review. Bioresource Technology, 97(9), 1061–1085. https://doi.org/10.1016/j.biortech.2005.05.001

8. de Morais Pinos, J.Y., de Melo, L.B., de Souza, S.D., Marçal, L., de Faria, E.H. 2022. Bentonite functionalized with amine groups by the sol-gel route as efficient adsorbent of rhodamine-B and nickel (II). Applied Clay Science, 223, 106494. https://doi.org/10.1016/j.clay.2022.106494

9. Funes, I.G.A., Peralta, M.E., Pettinari, G.R., Carlos, L., Parolo, M.E. 2020. Facile modification of montmorillonite by intercalation and grafting: The study of the binding mechanisms of a quaternary alkylammonium surfactant. Applied Clay Science, 195, 105738. https://doi.org/10.1016/j.clay.2020.105738

10. Gao, S., Wang, D., Huang, Z., Su, C., Chen, M., Lin, X. 2022. Recyclable NiO/sepiolite as adsorbent to remove organic dye and its regeneration. Scientific Reports, 12(1), 2895. https://doi.org/10.1038/s41598-022-06849-6

11. Gillman, P.K. 2011. CNS toxicity involving methylene blue: the exemplar for understanding and predicting drug interactions that precipitate serotonin toxicity. Journal of Psychopharmacology, 25(3), 429–436. https://doi.org/10.1177/0269881109359098

12. Gupta, V.K., Suhas, Ali, I., Saini, V.K. 2004. Removal of Rhodamine B, Fast Green, and Methylene Blue from Wastewater Using Red Mud, an Aluminum Industry Waste. Industrial & Engineering Chemistry Research, 43(7), 1740–1747. https://doi.org/10.1021/ie034218g

13. He, H., Chai, K., Wu, T., Qiu, Z., Wang, S., Hong, J. 2022. Adsorption of Rhodamine B from Simulated Waste Water onto Kaolin-Bentonite Composites. Materials, 15(12), 4058. https://doi.org/10.3390/ma15124058

14. Hidalgo-Herrador, J.M., Tišler, Z., Hajková, P., Soukupová, L., Zárybnická, L., Černá, K. 2017. Cold Plasma and Acid Treatment Modification Effects on Phonolite. Acta Chimica Slovenica, 598–602. https://doi.org/10.17344/acsi.2017.3343

15. Imgharn, A., Anchoum, L., Hsini, A., Naciri, Y., Laabd, M., Mobarak, M., Aarab, N., Bouziani, A., Szunerits, S., Boukherroub, R., Lakhmiri, R., Albourine, A. 2022. Effectiveness of a novel polyaniline@Fe-ZSM-5 hybrid composite for Orange G dye removal from aqueous media: Experimental study and advanced statistical physics insights. Chemosphere, 295, 133786. https://doi.org/10.1016/j.chemosphere.2022.133786

16. Inyinbor, A.A., Adekola, F.A., Olatunji, G.A. 2015. Adsorption of Rhodamine B dye from aqueous solution on Irvingia gabonensis biomass: Kinetics and thermodynamics studies. South African Journal of Chemistry, 68. https://doi.org/10.17159/0379-4350/2015/v68a17

17. Islam, M.R., Mostafa, M.G. 2022. Adsorption kinetics, isotherms and thermodynamic studies of methyl blue in textile dye effluent on natural clay adsorbent. Sustainable Water Resources Management, 8(2), 52. https://doi.org/10.1007/s40899-022-00640-1

18. Italiya, G., Ahmed, M.H., Subramanian, S. 2022. Titanium oxide bonded Zeolite and Bentonite composites for adsorptive removal of phosphate. Environmental Nanotechnology, Monitoring & Management, 17, 100649. https://doi.org/10.1016/j.enmm.2022.100649

19. Iwuozor, K.O. 2019. Prospects and Challenges of Using Coagulation-Flocculation Method in the Treatment of Effluents. In Advanced Journal of Chemistry-Section A, 2(2). http://ajchem-a.com

20. Jabar, J.M., Odusote, Y.A., Alabi, K.A., Ahmed, I.B. 2020. Kinetics and mechanisms of congo-red dye removal from aqueous solution using activated Moringa oleifera seed coat as adsorbent. Applied Water Science, 10(6), 136. https://doi.org/10.1007/s13201-020-01221-3

21. Jedli, H., Briki, C., Chrouda, A., Brahmi, J., Abassi, A., Jbara, A., Slimi, K., Jemni, A. 2019. Experimental and theoretical study of CO_2 adsorption by activated clay using statistical physics modeling. RSC Advances, 9(66), 38454–38463. https://doi.org/10.1039/C9RA05904K

22. Jović-Jovičić, N., Milutinović-Nikolić, A., Gržetić, I., Jovanović, D. 2008. Organobentonite as Efficient Textile Dye Sorbent. Chemical Engineering & Technology, 31(4), 567–574. https://doi.org/10.1002/ceat.200700421

23. Khattab, T.A., Abdelrahman, M.S., Rehan, M. 2020. Textile dyeing industry: environmental impacts and remediation. Environmental Science and Pollution Research, 27(4), 3803–3818. https://doi.org/10.1007/s11356-019-07137-z

24. Kloprogge, J.T. 2017. Raman and Infrared Spectroscopies of Intercalated Kaolinite Groups Minerals. In Developments in Clay Science, Elsevier B.V., 8, 343–410. https://doi.org/10.1016/B978-0-08-100355-8.00011-4

25. Kumar, A., Lingfa, P. 2020. Sodium bentonite and kaolin clays: Comparative study on their FT-IR, XRF, and XRD. Materials Today: Proceedings, 22, 737–742. https://doi.org/10.1016/j.matpr.2019.10.037

26. Liu, H., Liu, Z.-X., Yu, H.-R., Wang, Zhao, F., Wang, J. 2022. A hyper-cross-linked polymer derived from pitch as an efficient adsorbent for VOCs. High Performance Polymers, 34(8), 928–938. https://doi.org/10.1177/09540083221098159

27. Liu, Q., Wang, J., Duan, C., Wang, T., Zhou, Y. 2022. A novel cationic graphene modified cyclodextrin adsorbent with enhanced removal performance of organic micropollutants and high antibacterial activity. Journal of Hazardous Materials, 426, 128074. https://doi.org/10.1016/j.jhazmat.2021.128074

28. Maharana, M., Sen, S. 2021. Magnetic zeolite: A green reusable adsorbent in wastewater treatment. Materials Today: Proceedings, 47, 1490–1495. https://doi.org/10.1016/j.matpr.2021.04.370

29. Mahmoudabadi, T.Z., Talebi, P., Jalili, M. 2019. Removing Disperse red 60 and Reactive blue 19 dyes removal by using Alcea rosea root mucilage as a natural coagulant. AMB Express, 9(1), 113. https://doi.org/10.1186/s13568-019-0839-9

30. Malima, N.M., Owonubi, S.J., Lugwisha, E.H., Mwakaboko, A.S. 2021. Thermodynamic, isothermal and kinetic studies of heavy metals adsorption by chemically modified Tanzanian Malangali kaolin clay. International Journal of Environmental Science and Technology, 18(10), 3153–3168. https://doi.org/10.1007/s13762-020-03078-0

31. Malsawmdawngzela,R., liana,T., Tiwari,D. 2021. Sorption of Rhodamine B Dye onto Bentonite Clay-silane Composite Materials. Science & Technology Journal, 9(2), 161–168. https://doi.org/10.22232/stj.2021.09.02.20

32. Mao, H., Huang, Y., Luo, J., Zhang, M. 2021. Molecular simulation of polyether amines intercalation into Na-montmorillonite interlayer as clay-swelling inhibitors. Applied Clay Science, 202, 105991. https://doi.org/10.1016/j.clay.2021.105991

33. Menon, S., Agarwal, H., Shanmugam, V.K. 2021. Catalytical degradation of industrial dyes using biosynthesized selenium nanoparticles and evaluating its antimicrobial activities. Sustainable Environment Research, 31(1), 2. https://doi.org/10.1186/s42834-020-00072-6

34. Miyazaki, H., Kitano, Y., Makinose, Y., Handa, M., Nakashima, T. 2019. Synthesis Of Large-swelling Na-Type Bentonite By Hydrothermal Ion Eexchange. Clay Science, 23(3), 47–53. https://doi.org/10.11362/jcssjclayscience.23.3_47

35. Pai, S., Kini, M.S., Selvaraj, R. 2021. A review on adsorptive removal of dyes from wastewater by hydroxyapatite nanocomposites. Environmental Science and Pollution Research, 28(10), 11835–11849. https://doi.org/10.1007/s11356-019-07319-9

36. Pandey, S., Ramontja, J. 2016. Natural Bentonite Clay and Its Composites for Dye Removal: Current State and Future Potential. American Journal of Chemistry and Applications, 3(2), 8–19. http://www.openscienceonline.com/journal/ajca

37. Pironon, J., Pelletier, M., de Donato, P., Mosser-Ruck, R. 2003. Characterization of smectite and illite by FTIR spectroscopy of interlayer NH_4^+ cations. Clay Minerals, 38(2), 201–211. https://doi.org/10.1180/0009855033820089

38. Pourhakkak, P., Taghizadeh, M., Taghizadeh, A., Ghaedi, M. 2021. Adsorbent, 71–210. https://doi.org/10.1016/B978-0-12-818805-7.00009-6

39. Rápó, E., Aradi, L.E., Szabó, Á., Posta, K., Szép,R., Tonk,S. 2020. Adsorption of Remazol Brilliant Violet-5R Textile Dye from Aqueous Solutions by Using Eggshell Waste Biosorbent. Scientific Reports, 10(1), 8385. https://doi.org/10.1038/s41598-020-65334-0

40. Rehman, S.U., Yaqub, M., Noman, M., Ali, B., Ayaz Khan, M.N., Fahad, M., Muneeb Abid, M., Gul, A. 2019. The Influence of Thermo-Mechanical Activation of Bentonite on the Mechanical and Durability Performance of Concrete. Applied Sciences, 9(24), 5549. https://doi.org/10.3390/app9245549

41. Ribeiro dos Santos, F., de Oliveira Bruno, H.C., Zelayaran Melgar, L. 2019. Use of bentonite calcined clay as an adsorbent: equilibrium and thermodynamic study of Rhodamine B adsorption in aqueous solution. Environmental Science and Pollution Research, 26(28), 28622–28632. https://doi.org/10.1007/s11356-019-04641-0

42. Rochkind, M., Pasternak, S., Paz, Y. 2014. Using Dyes for Evaluating Photocatalytic Properties: A Critical Review. Molecules, 20(1), 88–110. https://doi.org/10.3390/molecules20010088

43. Salah, Gaber, Kandil. 2019. The Removal of Uranium and Thorium from Their Aqueous Solutions by 8-Hydroxyquinoline Immobilized Bentonite. Minerals, 9(10), 626. https://doi.org/10.3390/min9100626

44. Şenol, Z.M., Keskin, Z.S., Özer, A., Şimşek, S. 2022. Application of kaolinite-based composite as an adsorbent for removal of uranyl ions from aqueous solution: kinetics and equilibrium study. Journal of Radioanalytical and Nuclear Chemistry, 331(1), 403–414. https://doi.org/10.1007/s10967-021-08070-7

45. Shaarawy, H.H., Hussein, H.S., Kader, E.A., Hussien, N.H., Hawash, S.I. 2020. Adsorption performance of coated bentonite via graphene oxide. Bulletin of the National Research Centre, 44(1), 53. https://doi.org/10.1186/s42269-020-00299-8

46. Sharma, G., Sharma, S., Kumar, A., Lai, C.W., Naushad, Mu., Shehnaz, Iqbal, J., Stadler, F.J. 2022. Activated Carbon as Superadsorbent and Sustainable Material for Diverse Applications. Adsorption Science & Technology, 2022, 1–21. https://doi.org/10.1155/2022/4184809

47. Siregar, P.M.S.B.N., Normah, Juleanti, N., Wijaya, A., Palapa, N.R., Mohadi, R., Lesbani, A. 2021. Mg/Al-CH, Ni/Al-CH, and Zn/Al-CH as Adsorbents for Congo Red Removal in Aqueous Solution. Communications in Science and Technology, 6(2), 74–79.

48. Sudibandriyo, M., Putri, F.A. 2020. The Effect of Various Zeolites as an Adsorbent for Bioethanol Purification using a Fixed Bed Adsorption Column. International Journal of Technology, 11(7), 1300. https://doi.org/10.14716/ijtech.v11i7.4469

49. Taher, T., Mohadi, R., Lesbani, A. 2018. Effect of ti4+/clay ratio on the properties of titanium pillared bentonite and its application for Cr (VI) REMOVAL. Rasayan Journal of Chemistry, 11(3), 1244–1254. https://doi.org/10.31788/RJC.2018.1133065

50. Taher, T., Rohendi, D., Mohadi, R., Lesbani, A. 2019. Congo red dye removal from aqueous solution by acid-activated bentonite from sarolangun: kinetic, equilibrium, and thermodynamic studies. Arab Journal of Basic and Applied Sciences, 26(1), 125–136. https://doi.org/10.1080/25765299.2019.1576274

51. Teğin, İ., Saka, C. 2021. Chemical and thermal activation of clay sample for improvement adsorption capacity of methylene blue. International Journal of Environmental Analytical Chemistry, 1–12. https://doi.org/10.1080/03067319.2021.1928105

52. Tkaczyk, A., Mitrowska, K., Posyniak, A. 2020. Synthetic organic dyes as contaminants of the aquatic environment and their implications for ecosystems: A review. Science of The Total Environment, 717, 137222. https://doi.org/10.1016/j.scitotenv.2020.137222

53. Toor, M., Jin, B. 2012. Adsorption characteristics, isotherm, kinetics, and diffusion of modified natural bentonite for removing diazo dye. Chemical Engineering Journal, 187, 79–88. https://doi.org/10.1016/j.cej.2012.01.089

54. Varjani, S., Rakholiya, P., Ng, H.Y., You, S., Teixeira, J.A. 2020. Microbial degradation of dyes: An overview. Bioresource Technology, 314, 123728. https://doi.org/10.1016/j.biortech.2020.123728

55. Wang, L., Wang, M., Muhammad, H., Sun, Y., Guo, J., Laipan, M. 2022. Polypyrrole-Bentonite composite as a highly efficient and low cost anionic adsorbent for removing hexavalent molybdenum from wastewater. Journal of Colloid and Interface Science, 615, 797–806. https://doi.org/10.1016/j.jcis.2022.02.002

56. Wei, Q., Mcyotto, F.O., Chow, C.W.K., Nadeem, Z., Li, Z., Liu, J. 2020. Eco-friendly decolorization of cationic dyes by coagulation using natural coagulant Bentonite and biodegradable flocculant Sodium Alginate. SDRP Journal of Earth Sciences & Environmental Studies, 5(2), 51–60. https://doi.org/10.25177/jeses.5.2.ra.10648

57. Yang, L., Luo, X., Yan, L., Zhou, Y., Yu, S., Ju, H., Wang, Y., Zhang, L. 2022. Efficient selective adsorption of uranium using a novel eco-friendly chitosan-grafted adenosine 5′-monophosphate foam. Carbohydrate Polymers, 285, 119157. https://doi.org/10.1016/j.carbpol.2022.119157

58. Yoshida, Y., Shimada, T., Ishida, T., Takagi, S. 2020. Thermodynamic study of the adsorption of acridinium derivatives on the clay surface. RSC Advances, 10(36), 21360–21368. https://doi.org/10.1039/d0ra03158e

59. Zaher, M.S.A., Wahab, S.M.A., Taha, M.H.., Masoud, A.M. 2018. Sorption Characteristics of Iron, Fluoride and Phosphate from Wastewater of Phosphate Fertilizer Plant using Natural Sodium Bentonite. Journal of Membrane Science & Technology, 8(2). https://doi.org/10.4172/2155-9589.1000186

60. Zhong, M., Lao, Z., Tan, J., Yu, G., Liu, Y., Liang, Y. 2022. Synthesis of CoNi-layered double hydroxide on graphene oxide as adsorbent and construction of detection method for taste and odor compounds in smelling water. Journal of Hazardous Materials, 428, 128227. https://doi.org/10.1016/j.jhazmat.2022.128227